JPET Fast Forward. Published on December 2, 2005 as DOI: 10.1124/jpet.105.095463

JPET #95463

Inorganic mercury and methylmercury inhibit the $Ca_v3.1$ channel expressed in HEK 293 cells by different mechanisms.

Bohumila Tarabová, Martina Kurejová, Zdena Sulová, Melinda Drabová, Ľubica Lacinová

Institute of Molecular Physiology and Genetics, Slovak Academy of Sciences, Vlárska 5, 833 34 Bratislava, Slovakia (BT, MK, ZS, MD, LL)

JPET Fast Forward. Published on December 2, 2005 as DOI: 10.1124/jpet.105.095463
This article has not been copyedited and formatted. The final version may differ from this version.

JPET #95463

Inhibition of the $Ca_v3.1$ channel by Hg^{2+} and methylmercury.

Corresponding author: Ľubica Lacinová Institute of Molecular Physiology and Genetics, Slovak Academy of Sciences, Vlárska 5, 833 34 Bratislava, Slovakia

Fax +421-2-54773666

Phone +421-2-54772311

e-mail Lubica.Lacinova@savba.sk

Number of text pages: 35

Number of Tables: 1

Number of Figures: 10

Number of references: 22

Number of words in Abstract: 248

Number of words in Introduction: 713

Number of words in Discussion: 1522

Non-standard abbreviations:

MeHg – methyl mercury, HEK – human embryonic kidney, LVA – low voltage activated, HVA – high voltage activated, DRG – dorsal root ganglion, HP – holding potential, I-V – current-voltage, MTT - 3-(4,5-dimethylthiazol-2-yl)-2, 5-diphenyl tetrazolium bromide, MEM – minimal essential medium, FITC - fluorescein isothiocyanate, PI – propidium iodide, DMSO - dimethyl sulfoxide

Section assignment: Toxicology

Abstract

Part of the neurotoxic effects of inorganic mercury (Hg^{2+}) and methylmercury (MeHg) was attributed to their interaction with voltage-activated calcium channels. Effects of mercury on T-type calcium channels are controversial. Therefore we investigated effects of Hg^{2+} and MeHg on neuronal $Ca_v3.1$ (T-type) calcium channel stably expressed in HEK 293 cell line. Hg^{2+} acutely inhibited current through the $Ca_v3.1$ calcium channel in concentrations 10 nM and higher with an IC_{50} of 0.63±0.11 μM and a Hill coefficient of 0.73±0.08. Inhibition was accompanied by strong deceleration of current activation, inactivation and deactivation. The current-voltage relation was broadened and it's peak was shifted to a more depolarized membrane potentials by 1 μM of Hg^{2+}. MeHg in concentrations between 10 nM and 100 μM inhibited the current through the $Ca_v3.1$ calcium channel with an IC_{50} of 13.0±5.0 μM and a Hill coefficient of 0.47±0.09. Low concentration of MeHg (10 pM to 1 nM) had both positive and negative effects on the current amplitude. Micromolar concentrations of MeHg reduced the speed of current activation and accelerated current inactivation and deactivation. The current-voltage relation was not affected. Up to 72 hours exposure to 10 nM MeHg had no significant effect on current amplitude, while 72 hours long exposure to 1 nM MeHg increased significantly current density. Acute treatment with Hg^{2+} or MeHg did not affect HEK 293 cell viability. In conclusion, interaction with the $Ca_v3.1$ calcium channel may significantly contribute to neuronal symptoms of mercury poisoning during both acute poisoning and long-term environmental exposure.

Introduction

Mercury is a highly toxic heavy metal. Both methylmercury (MeHg) and inorganic mercury (Hg^{2+}) may cause accidental and occupational exposures and consequential damage in various organs in humans and animals (Clarkson et al., 2003). In humans, intoxication with mercury ions causes loss of coordination, decreased sensation, tremor and abnormal reflexes (Albers et al., 1988). These symptoms suggest that nervous system belongs to its primary targets. It was shown that in the brain Hg^{2+} inhibits synaptosomal Na^{+}-K^{+}-ATPase (Magour et al., 1987), blocks phosphorylation processes (Kuznetsov et al., 1987) and modulates mRNA metabolism (Kuznetsov and Richter, 1987).

Direct interaction with voltage- and ligand-gated ion channels may contribute to toxic effects of both methylmercury and inorganic mercury. Inhibition of neuronal sodium, potassium or calcium channels alters action potential shape and may result in the observed neuronal symptoms. Indeed, it was shown that an acute exposure to 1 μM or more of MeHg reduced potassium currents of cultured dorsal root ganglion cells (Leonhardt et al., 1996a). At least 10 μM Hg^{2+} was necessary for inhibition of potassium channels in outer hair cells (Liang et al., 2003). Sodium channels of cultured dorsal root ganglion cells were blocked by MeHg in concentrations above 10 μM (Leonhardt et al., 1996a). Among neuronal voltage-dependent ion channels, voltage dependent calcium channels are the most sensitive to mercury being acutely affected by its nanomolar concentrations (Shafer et al., 2002).

Effects of inorganic and/or organic mercury on voltage-dependent calcium channels were investigated in both native cell preparations and in recombinant expression systems. Results reported so far are partly controversial. Nanomolar concentrations of inorganic mercury increased the amplitude of high-voltage-activated (HVA) calcium current, presumably an L-type, in rat PC12 cells (Rossi et al., 1993). Micromolar concentrations of Hg^{2+} transiently increased low-voltage-activated (LVA) calcium current in rat hippocampal pyramidal cells (Szücs et al., 1997). In DRG neurons and in *Aplysia* neurons micromolar Hg^{2+} inhibited L, N and T-type calcium currents (Pekel et al., 1993).

MeHg was shown to inhibit both HVA and LVA calcium channels in native preparations. In rat hippocampal neurons HVA channels were less sensitive than LVA channels (Szücs et al., 1997). While some authors reported shift of current-voltage (I-V) relation by MeHg in the depolarising direction in DRG neurons (Leonhardt et al., 1996a; Leonhardt et al., 1996b), other authors did not observe any voltage dependence of current inhibition in granule cells (Sirois and Atchison, 2000). In addition to its effects on voltage-gated ion channels, inorganic mercury induced a background current in DRG neurons (Pekel et al., 1993) and organic mercury did so in rat Purkinje cells (Yuan and Atchison, 2005).

It is difficult to separate individual calcium channel types in native preparations. Therefore some authors investigated subtype-specific action of mercury on recombinant channels in an expression system. Until now, only the effects of mercury on recombinant HVA calcium channels were investigated. Micromolar concentrations of

MeHg inhibited the current through the $Ca_v1.2$ (L-type) calcium channel transiently expressed in human embryonic kidney cells (HEK 293) (Peng et al., 2002). Currents through the $Ca_v2.2$ (N-type) and $Ca_v2.3$ (R-type) calcium channels were inhibited by comparable concentrations of both Hg^{2+} and MeHg in the same expression system (Hajela et al., 2003).

Interaction of mercury with recombinant T-type calcium channels was not yet investigated. These channels are highly expressed in various neuronal tissues (for review see Lacinova, 2004) where they contribute to neuronal excitability, e.g., they generate low threshold calcium spikes or initiate burst firing. Therefore their modulation by mercury may significantly add to neuronal symptoms of mercury poisoning. In this study, we have compared the effects of Hg^{2+} and MeHg on $Ca_v3.1$ (T-type) calcium channel stably expressed in HEK 293 cells. Hg^{2+} was slightly more effective than MeHg in current inhibition. In addition, it affected the shape of I-V relation and decelerated kinetics of current gating. Furthermore, micromolar concentrations of inorganic mercury induced unspecific background current in HEK 293 cells. Effects of MeHg on current amplitude were more complex. Nanomolar concentrations caused both activation and inhibition of current amplitude. Organic mercury decelerated kinetics of channel activation while inactivation and deactivation were accelerated. The shape of I-V relation was not altered. Chronic application of 10 nM of MeHg caused minor increase in average current density. However, both forms of mercury did not have cytotoxic effects on HEK 293 cells.

JPET Fast Forward. Published on December 2, 2005 as DOI: 10.1124/jpet.105.095463
This article has not been copyedited and formatted. The final version may differ from this version.

Methods

Cell culture

Experiments were carried out on HEK 293 cells stably expressing the $Ca_v3.1$ subunit of T-type Ca^{2+} channel (CACNA1G). This gene has access number AJ012569 in the EMBL database. Construction of the expression vector was described previously (Klugbauer et al., 1999). HEK 293 line was purchased from DSMZ (Deutsche Sammlung von Mikroorganismen und Zellkulturen, GmbH, Braunschweig, Germany). The cells were grown in minimal essential medium (MEM) with Earle's salts, containing 10% (v/v) fetal calf serum, 100 U/ml penicillin - streptomycin, and 0.04% (w/v) G418 (geneticin, PAA Laboratories GmbH, Austria) at 37 °C in a humidified atmosphere of air: CO_2 95:5. The cells were harvested from their culture flasks by trypsinization and plated out 24 – 48 h before use in electrophysiological experiments. Background current activated by Hg^{2+} was analysed in nontransfected HEK 293 cells. Nontransfected cells were cultured as described above, except that G418 was absent in culture media.

Whole cell Ca^{2+} current recording

The extracellular solution contained (mM): N-methyl-D-glucamine, 160; $CaCl_2$, 2; $MgCl_2$, 1; HEPES (4-(2-hydroxyethyl)-1-piperazine-ethanesulphonic acid), 10; and glucose, 5; pH 7.4 (HCl). The intracellular solution contained (mM): CsCl, 130; EGTA (ethylene glycol-bis(β-aminoethyl ether)*N*,*N*,*N'*,*N'*-tetraacetic acid), 1; $MgCl_2$, 1; TEA-

Cl (tetra-ethyl ammonium chloride), 10; HEPES, 10; and Na-ATP (natrium adenosine triphosphate), 5; pH 7.4 (CsOH). All chemicals were obtained from Sigma. Osmolarity of the internal solution was approximately 300 mOsm. Osmolarity of the external solution was adjusted by adding glucose so that its final value was 2 – 3 mOsm below that of the internal solution. A 1 M stock solutions of both $HgCl_2$ and MeHg were prepared in deionized water every week, stored at 4°C and diluted in a bath solution prior to the experiment. Deionized water was made by Millipore Elix® Water Purification Systems. Extracellular solutions were exchanged by a gravity-driven flow system with manually controlled valves.

Ionic currents were recorded in the whole cell configuration of the patch clamp method using the HEKA-10 patch clamp amplifier (HEKA Electronic, Lambrecht, Germany). Patch-clamp pipettes were manufactured from borosilicate glass with the input resistance ranging from 1.8 to 2.1 MΩ. The capacitance of individual cells ranged between 10 and 22 pF. The series resistance ranged from 2.5 to 5 MΩ. Both capacitance and series resistance were compensated by built-in circuits of the HEKA-10 amplifier. The bath was grounded using an AgCl pellet connected to the experimental chamber through an agar bridge.

The holding potential (HP) in all experiments was –100 mV. The effect of mercurial salts was investigated using series of 40 ms long depolarizing pulses applied from the HP to the membrane potential of –30 mV with a frequency of 0.2 Hz. Current-voltage relations were measured by pulse protocol or by ramp protocol. Pulse protocol represented a series of 40 ms long depolarizing pulses applied every 3 s from the HP to

JPET Fast Forward. Published on December 2, 2005 as DOI: 10.1124/jpet.105.095463
This article has not been copyedited and formatted. The final version may differ from this version.

membrane potentials between –70 and +70 mV. Ramp protocol represented series of 100 ms long linear voltage ramps from –80 mV to +20 mV repeated every 3 s.

Cell survival rate tested with MTT assay

Nontransfected HEK 293 cells were plated onto 96-well plates (1×10^4 cells/well) and cultured overnight to allow for cell attachment. Cells were then incubated with control MEM, MEM containing 10 μM of MeHg or MEM containing 1 μM Hg^{2+} for 10 minutes or for 4 hours. After incubation cells were centrifuged, 200 μl of fresh MEM containing 10 μl of MTT (3[4,5-dimethylthiazol-2-yl]-2,5-diphenyltetrazolium bromide; 5 mg/ml) were added and incubated for further three hours and centrifuged again. The supernatant was discarded and the pellet was dissolved in 150 μl of DMSO (dimethyl sulfoxide). The optical density at 540 nm was recorded on a MicroQuant Microplate Spectophotometer (Biotek, USA). Cell viability was determined relative to untreated controls.

Detection of cell viability and apoptotic cells

Cell viability and apoptosis were measured by annexin V-fluorescein isothiocyanate (FITC) and propidium iodide (PI) staining using the Annexin V-FITC Apoptosis Detection Kit (Sigma). Approximately 1×10^6 of nontransfected HEK 293 cells/ml were incubated in the control medium, in a medium with 10 μM of MeHg or in medium with 1 μM of Hg^{2+} for 10 minutes or for 4 hours. After the indicated time cells were harvested, washed twice with PBS and stained with annexin V-FITC and PI according

JPET Fast Forward. Published on December 2, 2005 as DOI: 10.1124/jpet.105.095463
This article has not been copyedited and formatted. The final version may differ from this version.

to manufacturer's instructions. The cells were then analyzed using a Coulter Epics Altra flow cytometer (Beckman Coulter, USA).

Data analysis

Data were recorded using a HEKA Pulse 8.5 program and analysed with HEKA Pulsefit 8.5 and Origin 7.5 software. Capacity transients and series resistance were compensated on-line by procedures built in the EPC 10 amplifier. The currents measured during Hg^{2+} application were corrected for linear time-independent component of the leak current, which was calculated individually for each current trace according to the equation (1):

$$I_{sub} = I(V_{membr}) - \frac{I(h)}{(-100)} * V_{membr} \qquad (1)$$

where I_{sub} is leak-subtracted current, $I(V_{membr})$ is nonsubtracted current measured at the membrane potential V_{membr}, I(h) is the average membrane current measured during the holding potential of –100 mV and V_{membr} is the membrane potential.

Concentration dependencies were fitted by the Hill equation (2):

$$\frac{I}{I_0} = \frac{1}{1 + \left(\frac{[\text{mercury}]}{IC_{50}}\right)^n} \qquad (2)$$

where I and I_0 are calcium current amplitudes measured in the presence and absence of mercury, respectively, [mercury] is the concentration of particular form of mercury, IC_{50} is the half-maximal inhibitory concentration and *n* is the Hill coefficient. Significance of the observed effects was assessed by paired or non-paired Student t-test, as appropriate.

Values of $p < 0.05$ were considered to be significant. All experimental values are expressed as mean±SEM.

Results

Background current activated by inorganic mercury

During initial experiments with inorganic mercury (Hg^{2+}) rapid increase of a background current in the presence of micromolar mercury concentration was observed. For clear definition of experimental conditions an analysis of this phenomenon was necessary. Nontransfected HEK 293 cells were used for these experiments. Amplitude of the leak current was concentration dependent and started to increase immediately after application of suprathreshold concentrations of Hg^{2+}. The current was activated by the ramp protocol. Small constant leak current with an average amplitude bellow 5 pA/pF at a membrane potential of -80 mV was observable in cells exposed to constant flow of the control solution (not shown) or to 10 nM of Hg^{2+} (Figure 1a). The threshold concentration for an activation of the Hg^{2+}-dependent background current was 100 nM. This concentration caused gradual increase in the membrane current amplitude, which started almost immediately after switching to perfusion by Hg^{2+} – containing solution and saturated after 200 s. At higher concentrations no saturation of the background current amplitude was reached during 6 min long application. Current-voltage (I-V) relation measured by voltage ramp protocol (Figure 1b) revealed a purely linear character of the membrane current measured under the control conditions. The linear I-V is characteristic for a non-specific leak current. In the presence of 1 μM Hg^{2+} the I-V relation was strongly outwardly rectifying. Such voltage course is characteristic for current carried through voltage-dependent ion channels. Nevertheless, the I-V relation in the presence of Hg^{2+} retained linear voltage course for membrane voltages between –

80 mV and –20 mV. Background currents were essentially time independent under the control conditions and in the presence of Hg^{2+} (Figures 1c and d). Therefore it was justifiable to use the linear leak subtraction method for the analysis of currents activated by depolarizing pulses to –30 mV.

Hg^{2+} inhibits calcium current through the $Ca_v3.1$ channel in concentration-dependent manner

Inorganic mercury in concentrations ranging from 10 nM to 100 μM inhibited the calcium current through the expressed $Ca_v3.1$ channels (Figures 2a-d). All analyses of experimental data were performed on recordings corrected for linear leak component. Effect of 10 nM Hg^{2+} was negligible. Inhibition of the current amplitude increased with increasing Hg^{2+} concentration and was nearly complete at a concentration of 100 μM. The block was virtually irreversible at low concentrations, but was partly reversible at higher concentrations. At a concentration of 100 μM the reversibility of Hg^{2+} effect was not tested because of rapid increase in background current, which eventually led to loss of the proper whole cell clamp. Fit of experimental data by Hill equation resulted in an IC_{50} = 0.63±0.11 μM and a Hill coefficient n = 0.73±0.08.

Hg^{2+} slows kinetics of the calcium current through the $Ca_v3.1$ channel and alters its voltage dependence

Visual inspection of current recordings presented in the Figure 2c suggested that in addition to amplitude inhibition, Hg^{2+} slowed all processes underlying the gating of the

$Ca_v3.1$ channel, i.e., activation, inactivation and deactivation. In order to quantify this phenomenon current trace were fitted by Hodgkin-Huxley equation in the m2h form. The threshold concentration for all changes in channel kinetics was 100 nM. The activation time constant increased with increasing Hg^{2+} concentration (Figure 3a). The inactivation time constant increased to such an extent that at the concentration of 10 μM Hg^{2+} current was virtually non-inactivating and current traces could not be satisfyingly fitted (Figures 2c and 3b). A single exponential curve fit the time course of the tail current. In contrast to activation and inactivation time constants, an increase in time constants of current deactivation saturated at the concentration of 1 μM Hg^{2+} (Figure 3c).

Effect of Hg^{2+} on the position of the peak of I-V relation and on the shape of I-V relation was investigated using a 100 ms long voltage ramp. Ramp protocol was preferred to a series of depolarizing pulses in these experiments. As demonstrated in the Figure 1, higher concentrations of Hg^{2+} caused a rapid increase in the background current and therefore subtraction of the linear leak component provided more credible results when applied to rapid ramp protocol. 100 nM of Hg^{2+} did not shift the peak or altered the shape of I-V relation (data not shown). Concentration of 1 μM shifted the peak of I-V to more depolarized voltages and increased its width (Figures 4 a and b). At higher Hg^{2+} concentrations rapid increase in the background current precluded analysis of the I-V relation.

MeHg has a dual effect on the calcium current through the $Ca_v3.1$ channel

JPET Fast Forward. Published on December 2, 2005 as DOI: 10.1124/jpet.105.095463
This article has not been copyedited and formatted. The final version may differ from this version.

Action of the organic mercury on the $Ca_v3.1$ channel differed from the effects of inorganic mercury in virtually all aspects. No background current was activated even at the highest tested MeHg concentration of 100 μM. The threshold for the functional interaction of MeHg with the channel was as low as 10 pM. While concentrations of 10 nM and higher simply inhibited the calcium current (Figures 5 a, b and f), lower concentrations caused a dual effect: either a sole inhibition was observed in some cells and a sole activation in others (Figures 5 c and d), or an initial potentiation of the current was followed by inhibition (Figure 5 e). Ostentation and inhibition caused by 10 pM to 1 nM of MeHg were evaluated separately (Figure 5f). Data describing the inhibition of the calcium current were fitted by Hill equation with an IC_{50} = 13.0±5.0 μM and a Hill coefficient n = 0.47±0.09.

MeHg alters kinetics of the calcium current through the $Ca_v3.1$ channel but not its voltage dependence

Simple visual inspection of the current traces presented in the Figure 5 suggested that the MeHg effects on gating kinetics were less prominent than the effects of Hg^{2+}. Only micromolar concentrations of MeHg altered significantly the time constants of activation, inactivation and deactivation. The extent of deceleration of the current activation was smaller that the extent of deceleration by Hg^{2+}. In addition, 10 μM of MeHg caused transient acceleration of an activation kinetics, which was followed by a final deceleration (Figure 6a). In contrast to the effect of Hg^{2+}, MeHg accelerated significantly current inactivation (Figure 6b) and deactivation (Figure 6c). Time

constants evaluated for different pools of cells under the control conditions varied slightly, but the differences between them were not statistically significant.

Absence of background current activation allowed using a set of depolarizing pulses for the analysis of I-V relation. Neither the shape of I-V relation nor the voltage at which the current reached the maximum were affected by the presence of MeHg (Figures 7 a and b).

Chronic exposure to nanomolar MeHg enhances the calcium current through the $Ca_v3.1$ channel

Long-term effects of MeHg on the current through the $Ca_v3.1$ channel were analyzed after 24 hours and 72 hours long exposures to 1 nM and 10 nM of MeHg. Cells were cultured in parallel in control MEM and in MEM with added MeHg. At the end of the test period cells were transferred into the bath solution with or without the respective concentration of MeHg. I-V relations for 15 cells cultured under each condition were measured using the pulse protocol, averaged and compared. Long-term presence of MeHg slightly altered the current amplitudes without shifting peak or altering shape of the I-V relation (Figures 8 a and b). The current amplitude activated by the depolarization to –30 mV (peak of the I-V relation) was potentiated by 1 nM of MeHg. The potentiation was significant after 72 hours long exposure (Figure 8 c). 10 nM of MeHg inhibited slightly, but insignificantly current amplitude (Figure 8c). Kinetics of current activation, inactivation and deactivation was not changed (data not shown).

JPET Fast Forward. Published on December 2, 2005 as DOI: 10.1124/jpet.105.095463
This article has not been copyedited and formatted. The final version may differ from this version.

Effects of Hg^{2+} and MeHg on cell viability

Rapid increase in background current observed upon cell exposure to Hg^{2+} could be explained by cytotoxic effects of mercury leading to an increase in membrane permeability and eventually to the cell death. Viability of HEK 293 cells stably expressing the $Ca_v3.1$ channel was determined using the colorimetric MTT test. As shown in the Figure 9, 10 min long treatment with 10 μM MeHg or 1 μM Hg^{2+} did not cause significant increase in cell death. After 4 hours incubation a significant ($p<0.001$) increase in the cell death was observed in the cells treated with 1 μM Hg^{2+}, but not in those treated with 10 μM MeHg.

In order to distinguish apoptotic and necrotic cells, annexin V-FITC and PI staining detected by flow cytometry were used. HEK 293 cells stably expressing the $Ca_v3.1$ channel were treated with control MEM, 10 μM MeHg or 1 μM Hg^{2+} for 10 min or for 4 hours. No increase in the number of apoptotic or necrotic cells was observed (Figure 10). Under all conditions, the majority of cells (66-70%) were found in the lower left quadrant (viable cells). The upper right quadrant corresponding to late apoptosis and necrosis contained approximately16-20% of all cells and represented the cells damaged during passaging. Minor proportions of cells were found in lower right quadrant (necrosis) and negligible amount of the cells were located in upper left quadrant (early apoptosis). Distribution of cells among the quadrants was not apparently altered by mercury treatments (Figure 10). The increase in the cell death observed in the cells treated for 4 hours with 1μm Hg^{2+} with the MTT assay (Figure 9) may be attributed to cell necrosis rather that to cell apoptosis.

Discussion

In this study we report for the first time the effects of methylmercury and mercury on low-voltage activated neuronal $Ca_v3.1$ calcium channels investigated in expression system. So far, the interaction of Hg^{2+} with neuronal low-voltage activated (LVA) calcium channels was investigated in native systems only. The main advantage of using channels expressed in HEK 293 cells is the possibility to study single channel type in isolation. This is especially important in the case of LVA calcium channels, which in native system are superimposed by several-fold higher current density of calcium current carried through high-voltage activated calcium channels. Furthermore, we have used the cell line stably expressing the channel instead of transiently transfected cells. In addition to acute effects, stable cell line enabled investigation of effects of long-term exposure to mercurials on $Ca_v3.1$ channel in isolation. Certain drawback of use of non-native system is a lack of certain reaction pathways involved into neurotoxicity of mercurials in the native systems. Therefore our study is limited to the investigation of direct effects of mercurials on the $Ca_v3.1$ calcium channel.

Both mercurials inhibited the current through the expressed $Ca_v3.1$ calcium channel in concentrations above 10 nM. Inorganic mercury was approximately 20-fold more potent inhibitor of T-type calcium current than methylmercury. IC_{50} of 0.63 μM found in our study for Hg^{2+} corresponds to that reported by the groups of Pekel and Leonhardt for T-type current in rat dorsal root ganglion (DRG) neurons (Pekel et al., 1993; Leonhardt et al., 1996b). IC_{50} close to 1 μM of Hg^{2+} is also similar to those reported for HVA calcium channels (for review see Atchison, 2003). In contrast, Szücs and coauthors

found dual effect of Hg^{2+} on low-voltage activated calcium channel in cultured rat hippocampal neurons (Szücs et al., 1997). His study identified the type of observed calcium channel solely on the basis of its activation potential. The potentiating effect of Hg^{2+} in hippocampal cells might have been mediated by another subtype of LVA calcium channel, i.e., $Ca_v3.2$ or $Ca_v3.3$, whose expression level in rat hippocampus is high (for review see Lacinova, 2004). Alternatively, potentiation seen by these authors may be mediated by HVA calcium channels, e.g., $Ca_v2.3$ or $Ca_v1.3$, which could be activated at voltages of –20 mV and –10 mV, used in Szücs' experiments. This interpretation is supported by the report of Rossi and coauthors, who found an enhancement of calcium current by Hg^{2+} in this depolarization range in PC12 cells and attributed it to the effect on L-type calcium channel (Rossi et al., 1993).

In our study only the MeHg had dual effect on calcium current through the $Ca_v3.1$ channel. This effect was observed at picomolar concentrations and was combined with an inhibitory effect. Similar observation was made by Szücs in hippocampal neurons. In these experiments micromolar concentration of MeHg was used (Szücs et al., 1997). Shift in concentration dependence of MeHg effect could be explained, as we suggested in the case of Hg^{2+} effect, by different subtype of LVA calcium channel. Additionally, 10 mM of Ca^{2+} was used in Szücs' experiments, while we have used 2 mM Ca^{2+}. If calcium competes with mercury for binding site in the channel, enhanced calcium concentration would shift dose-response curve towards higher concentrations. 1000-fold increase in MeHg concentration at which current potentiation could be seen is too big to consider solely this effect as an explanation. Therefore subtype specificity may be a more important factor.

Increase of calcium current in the presence of low concentrations of MeHg is unique to LVA calcium channels. No such effect was observed in HVA calcium channels (Atchison, 2003). Because of its transient nature during acute application this effect may be of importance during chronic environmental exposure rather than during acute poisoning. Indeed, 72 hours long exposure to 1 nM of MeHg enhanced significantly the averaged current amplitude. This result support and extends our observation that low concentrations of MeHg caused dual acute effect on the current amplitude. Apparently, in chronic experiment current potentiation by 1 nM of MeHg overwhelmed the current inhibition. When concentration was increased to 10 nM, current inhibition was more potent. The observed decrease of the calcium current amplitude was in agreement with the study made by Shaffer and co-authors on HVA calcium channels in PC12 cells (Shafer et al., 2002). Nevertheless, the decrease in current amplitude observed in our experiments was not significant. Furthermore, IC_{50} for acute current inhibition by MeHg was 10 to 20-fold higher than those found for HVA calcium channels in native tissue (Shafer and Atchison, 1991; Leonhardt et al., 1996a; Leonhardt et al., 1996b; Sirois and Atchison, 2000) or in an expression system (Peng et al., 2002; Hajela et al., 2003). Therefore we may conclude that LVA $Ca_v3.1$ calcium channel is generally less sensitive to MeHg than HVA calcium channels are. Leonhardt reported similar sensitivity of LVA and HVA calcium channels in DRG neurons to MeHg (Leonhardt et al., 1996b), however, in his work he did not distinguish between channel subtypes.

In agreement with reports on native or expressed HVA or LVA calcium channels the inhibition of the $Ca_v3.1$ calcium channel by MeHg was irreversible. In contrast,

activation of the current by low MeHg concentration reversed readily upon washout. This observation suggests, that both effects are mediated by interaction with different interaction sites and/or by different mechanisms. Existence of two interaction sites for MeHg is supported also by dual effect of its picomolar concentrations on the current amplitude and by low steepness of dose–response relationship. Inhibition by Hg^{2+} was partly reversible at higher mercury concentrations. Reversibility may be highly selective for channel subtypes, because it was observed for $Ca_v2.2$, but not for $Ca_v2.3$ channels expressed in HEK 293 cells (Hajela et al., 2003).

Reports on voltage dependence of interaction of mercurials with calcium channels are controversial. Most authors did not find any voltage dependence for Hg^{2+} (Busselberg et al., 1994) or MeHg (Sirois and Atchison, 2000; Peng et al., 2002; Hajela et al., 2003) interaction with HVA calcium channels. In contrast, Leonhardt found a shift of I-V relation towards more depolarized membrane potentials upon exposure of DRG cells to both Hg^{2+} and MeHg (Leonhardt et al., 1996b). The calcium current measured from DRG neurons does include LVA calcium current. In our study a similar shift of I-V was found for Hg^{2+} only. Additionally, the I-V relation was not only shifted but also widened, or, in other words, the slope factor for dependence of current amplitude on membrane depolarization was enhanced. This observation suggests that Hg^{2+} interferes with the channels activation and/or inactivation gate. In agreement with this suggestion Hg^{2+} slowed down significantly kinetics of channel activation, inactivation and deactivation.

MeHg altered channel kinetics in concentrations, which caused inhibition of the calcium current. These effects were partly opposite to the effects of Hg^{2+} on the calcium current. MeHg accelerated channel inactivation and deactivation while it slowed down the channel activation in parallel to the effect of Hg^{2+} on the activation. Such effects suggest an interaction of MeHg with an open channel state. This explanation is in line with findings, that inhibition of calcium current by MeHg is frequency-dependent (Sirois and Atchison, 2000; Peng et al., 2002).

The finding that Hg^{2+} activates long lasting inward current at higher concentrations corresponds with reports on DRG neurons (Pekel et al., 1993; Leonhardt et al., 1996b). This current is specific for certain cell types, as it was not observed in *Aplysia* neurons (Pekel et al., 1993). The channel responsible for this current was not identified, but we may hypothesize that it is a chloride-permeable channel, as the current activation was not affected by replacement of NaCl by NMDG-Cl in extracellular solution (Lacinova et al., unpublished data).

An alternative explanation for the increased background conductance may be an increase in the permeability of the cell membrane due to cytotoxic effects of Hg^{2+}. We have tested for apoptotic and necrotic cell death using MTT assay and flow cytometry. No cytotoxic effects of any form of mercury were detected after 10 min long treatment, corresponding to the typical length of electrophysiological experiment. Minor but significant cell death most probably due to necrosis was observed after 4 hours treatment with 1 μM of Hg^{2+}. This could not interfere with electrophysiological experiments and their interpretations.

In conclusion, both MeHg and Hg^{2+} inhibited current through the $Ca_v3.1$ calcium channel at low micromolar concentration. Therefore this interaction may significantly contribute to pathology of acute mercury poisoning. T-type calcium channels may generate a low-threshold calcium spike, which play an important role in the genesis of burst firing (Perez-Reyes, 2003). Because these channels are preferentially localized to dendrites, their inhibition may interfere with dendritic signal amplification. In thalamic neurons T-type currents play an important role in oscillatory behavior (for review see Perez-Reyes, 2003). Therefore their suppression may lead to inappropriate oscillations of these circuits, or thalamocortical dysrhythmias. A prolonged exposure to nanomolar concentrations of MeHg perturbs the channel function. These effects may increase Ca^{2+} entry through the T-type channels, contribute to spike repolarization and afterhyperpolarizations and eventually might lead to overexcitability in various neuronal tissues. A long exposure to low mercury concentrations may thus contribute to pathology of chronic poisoning.

Acknowledgements

Authors thank Stanislava Manová, Mário Šereš and Lenka Gibalová for skilful technical assistance, Ján Sedlák and Branislav Uhrík for valuable discussion and Anthony Gioio for helpful comments on manuscript.

References

Albers JW, Kallenbach LR, Fine LJ, Langolf GD, Wolfe RA, Donofrio PD, Alessi AG, Stolp-Smith KA and Bromberg MB (1988) Neurological abnormalities associated with remote occupational elemental mercury exposure. *Ann Neurol* **24**:651-659.

Atchison WD (2003) Effects of toxic environmental contaminants on voltage-gated calcium channel function: from past to present. *J Bioenerg Biomembr* **35**:507-532.

Busselberg D, Platt B, Michael D, Carpenter DO and Haas HL (1994) Mammalian voltage-activated calcium channel currents are blocked by Pb^{2+}, Zn^{2+}, and Al^{3+}. *J Neurophysiol* **71**:1491-1497.

Clarkson TW, Magos L and Myers GJ (2003) The toxicology of mercury--current exposures and clinical manifestations. *N Engl J Med* **349**:1731-1737.

Hajela RK, Peng SQ and Atchison WD (2003) Comparative effects of methylmercury and Hg^{2+} on human neuronal N- and R-type high-voltage activated calcium channels transiently expressed in human embryonic kidney 293 cells. *J Pharmacol Exp Ther* **306**:1129-1136.

Klugbauer N, Marais E, Lacinova L and Hofmann F (1999) A T-type calcium channel from mouse brain. *Pflugers Arch* **437**:710-715.

Kuznetsov DA and Richter V (1987) Modulation of messenger RNA metabolism in experimental methyl mercury neurotoxicity. *Int J Neurosci* **34**:1-17.

Kuznetsov DA, Zavijalov NV, Govorkov AV and Sibileva TM (1987) Methyl mercury-induced nonselective blocking of phosphorylation processes as a possible cause of protein synthesis inhibition in vitro and in vivo. *Toxicol Lett* **36**:153-160.

Lacinova L (2004) Pharmacology of recombinant low-voltage activated calcium channels. *Curr Drug Targets CNS Neurol Disord* **3**:105-111.

Leonhardt R, Haas H and Busselberg D (1996a) Methyl mercury reduces voltage-activated currents of rat dorsal root ganglion neurons. *Naunyn Schmiedebergs Arch Pharmacol* **354**:532-538.

Leonhardt R, Pekel M, Platt B, Haas HL and Busselberg D (1996b) Voltage-activated calcium channel currents of rat DRG neurons are reduced by mercuric chloride ($HgCl_2$) and methylmercury (CH_3HgCl). *Neurotoxicology* **17**:85-92.

Liang GH, Jarlebark L, Ulfendahl M and Moore EJ (2003) Mercury (Hg^{2+}) suppression of potassium currents of outer hair cells. *Neurotoxicol Teratol* **25**:349-359.

Magour S, Maser H and Greim H (1987) The effect of mercury chloride and methyl mercury on brain microsomal Na^+-K^+-ATPase after partial delipidisation with Lubrol. *Pharmacol Toxicol* **60**:184-186.

Pekel M, Platt B and Busselberg D (1993) Mercury (Hg^{2+}) decreases voltage-gated calcium channel currents in rat DRG and Aplysia neurons. *Brain Res* **632**:121-126.

Peng S, Hajela RK and Atchison WD (2002) Effects of methylmercury on human neuronal L-type calcium channels transiently expressed in human embryonic kidney cells (HEK-293). *J Pharmacol Exp Ther* **302**:424-432.

Perez-Reyes E (2003) Molecular physiology of low-voltage-activated T-type calcium channels. *Physiol Rev* **83**:117-161.

Rossi AD, Larsson O, Manzo L, Orrenius S, Vahter M, Berggren PO and Nicotera P (1993) Modifications of Ca^{2+} signaling by inorganic mercury in PC12 cells. *FASEB J* **7**:1507-1514.

Shafer TJ and Atchison WD (1991) Methylmercury blocks N- and L-type Ca^{2+} channels in nerve growth factor-differentiated pheochromocytoma (PC12) cells. *J Pharmacol Exp Ther* **258**:149-157.

Shafer TJ, Meacham CA and Barone S, Jr. (2002) Effects of prolonged exposure to nanomolar concentrations of methylmercury on voltage-sensitive sodium and calcium currents in PC12 cells. *Brain Res Dev Brain Res* **136**:151-164.

Sirois JE and Atchison WD (2000) Methylmercury affects multiple subtypes of calcium channels in rat cerebellar granule cells. *Toxicol Appl Pharmacol* **167**:1-11.

Szücs A, Angiello C, Salanki J and Carpenter DO (1997) Effects of inorganic mercury and methylmercury on the ionic currents of cultured rat hippocampal neurons. *Cell Mol Neurobiol* **17**:273-288.

Yuan Y and Atchison WD (2005) Methylmercury induces a spontaneous, transient slow inward chloride current in purkinje cells of rat cerebellar slices. *J Pharmacol Exp Ther* **313**:751-764.

Footnotes

Supported by grants from Volkswagen Stiftung, VEGA 2/4009 and APVT-51-027404.

Address for reprint requests: Ľubica Lacinová, Institute of Molecular Physiology and Genetics, Slovak Academy of Sciences, Vlárska 5, 833 34 Bratislava, Slovakia

Fax +421-2-54773666

e-mail lubica.lacinova@savba.sk

JPET Fast Forward. Published on December 2, 2005 as DOI: 10.1124/jpet.105.095463
This article has not been copyedited and formatted. The final version may differ from this version.

Legends to Figures

Figure 1

Background current induced by inorganic mercury in non-transfected HEK 293 cells. The current was activated by 100 ms long voltage ramps from the membrane potential of –80 mV to +80 mV applied each 3 s. (a) Current amplitudes were evaluated from voltage ramps at a potential of –80 mV. Hg^{2+} application is marked by an arrow. The following number of cells were averaged for individual Hg^{2+} concentrations: 10 nM, n = 3; 100 nM, n = 5; 1 μM, n = 8; 10 μM, n = 4. (b) Current-voltage (I-V) relations measured by voltage ramp protocol under the control conditions and after 200 s of presence of 1 μM Hg^{2+}. (c) Current traces measured in the control bath solution by a series of 100 ms long depolarizing pulses from a holding potential (HP) of –100 mV to voltages between –70 mV and +50 mV. (d) Current traces measured after 200 s of presence of 1 μM Hg^{2+} by the same voltage protocol as in the panel c.

Figure 2

Inhibition of the $Ca_v3.1$ calcium channel by inorganic mercury. The current was activated by a train of depolarizing pulses applied from a HP of –100 mV to –30 mV with a frequency of 0.2 Hz. Hg^{2+} application is marked by filled symbols and an arrow. Starts of Hg^{2+} washout are marked by filled symbols. Numbers of cells averaged for individual Hg^{2+} concentrations are as follow: (a) 10 nM, n = 4; 100 nM, n = 6; 1 μM, n = 8; (b) 10 μM, n = 5; 100 μM, n = 6. (c) Examples of current traces measured during pulses marked in panels (a) and (b) by filled symbols in the absence (solid line) or presence (dashed line) of Hg^{2+}. The linear component of the leak current is subtracted

from the raw data. (d) Concentration dependence of the inhibition of current amplitude. Solid line represents a fit of experimental data by the Hill equation with an IC_{50} of 0.63±0.11 μM and a Hill coefficient of 0.73±0.08.

Figure 3

Hg^{2+} slowed the kinetics of the currents through the $Ca_v3.1$ channel. Time constants were evaluated from the data presented in the Figure 2. Open bars represent time constant calculated from the current traces recorded just before Hg^{2+} application. Filled bars correspond to the time constants calculated from the current traces recorded just before the start of Hg^{2+} washout. Time constants of current activation and inactivation were evaluated from the fit of current traces by m2h form of Hodgkin-Huxley equation. (a) Time constants of current activation. (b) Time constants of current inactivation. (c) Deactivation time constants were estimated from monoexponential fits of tail currents. The significance of difference between two data sets (control vs. Hg^{2+}) was evaluated by the paired Student's t-test. ** - $p < 0.01$, *** - $p < 0.001$.

Figure 4

Hg^{2+} shifted the I-V relation of the current through the $Ca_v3.1$ channel. I-V relations were measured by a series of 100 ms long voltage ramps from the membrane potential of –80 mV to +20 mV. (a) Currents recorded just before application of 1 μM Hg^{2+} (solid line) and after 150 s of its presence (dashed line). (b) For a better comparison, traces from the panel (a) were normalized to the maximal current amplitude.

JPET Fast Forward. Published on December 2, 2005 as DOI: 10.1124/jpet.105.095463
This article has not been copyedited and formatted. The final version may differ from this version.

Figure 5

Inhibition and potentiation of the current through the $Ca_v3.1$ channel by MeHg.

The current was activated by a train of depolarizing pulses applied from a HP of –100 mV to –30 mV with a frequency of 0.2 Hz. (a) Time course of the inhibition of current amplitude by intermediate to high MeHg concentrations. An arrow marks the moment of Hg^{2+} application. Numbers of cells averaged for individual Hg^{2+} concentrations were as follow: 100 nM, n = 10; 1 μM, n = 11; 10 μM, n = 6; 100 μM, n = 6. (b) Examples of current traces measured during a train of depolarizing pulses in the absence (solid line) or presence (dashed line) of each concentration of MeHg. (c) An example of the current inhibition by 100 pM of MeHg. Solid line indicates the presence of MeHg in the bath solution. The moments of MeHg application and washout are indicated by filled symbols. Examples of current traces are shown in the inset and numbers indicates the times when they were recorded. (d) An example of the current potentiation by 100 pM of MeHg. Solid line indicates the presence of MeHg in the bath solution. The moments of MeHg application and washout are indicated by filled symbols. Examples of current traces are shown in the inset and numbers indicates the time points when they were recorded. (e) An example of a dual effect of the low concentration of MeHg on the current amplitude. Solid line indicates the presence of MeHg in the bath solution. The points of MeHg application and washout are indicated by filled symbols. Examples of current traces are shown in the inset and numbers indicates the time points when they were recorded. (f) Concentration dependence of the inhibition and potentiation of current amplitude. Open symbols represent positive effect of MeHg on the calcium current amplitude and filled symbols represent current inhibition. For 100 pM of MeHg activation and inhibition were evaluated for distinct cells, for 10 pM and 1 nM both

effects were estimated on the same cells. Numbers written next to each point represent the numbers of cells averaged. Dashed lines are simple connectors of experimental data. Solid line represents a fit of inhibition data by the Hill equation. Scale bars in all panels represent 10 ms (horizontal) and 500 pA (vertical).

Figure 6

MeHg slowed the kinetics of the current activation and accelerated its inactivation and deactivation. Time constants were calculated from the data presented in the Figure 5a just before MeHg application (open bars) and just before the start of MeHg washout (filled bars). (a) Time constants of current activation were evaluated from the fit of current traces by m2h form of Hodgkin-Huxley equation. (b) Time constants of current inactivation were evaluated by the same method as in panel (a). (c) Deactivation time constants were estimated from monoexponential fits of tail currents. The significance of difference between two data sets was evaluated by the paired Student's t-test. ** - $p < 0.01$, *** - $p < 0.001$.

Figure 7

MeHg does not affect the shape of I-V relation. (a) I-V relations were measured by series of depolarizing pulses from a HP of –100 mV to indicated voltages before (open symbols, control conditions, n = 10) and after (filled symbols, 10 μM MeHg, n = 10) pulse protocols presented in the Figure 5a. (b) Data from the panel (a) were normalized to a peak amplitude of each I-V relation to facilitate the comparison.

Figure 8

Chronic application of MeHg has minor effects on the current through the $Ca_v3.1$ calcium channel. (a) I-V relations were measured by series of depolarizing pulses from a HP of –100 mV to indicated voltages. Open symbols represent an averaged I-V from 15 cells cultured for 72 hours under control conditions. Filled symbols represent an averaged I-V from 15 cells cultured for 72 hours in the presence of 1 nM MeHg. (b) Data from the panel (a) were normalized to peak amplitude of each I-V relation to facilitate the comparison. (c) Averaged current densities measured from 15 cells during depolarizing pulses from HP of –100 mV to –30 mV (the peaks of I-V relations shown in panels a and b). Cells were cultured in parallel in DMEM (open bars) and in the presence of 1 nM (hatched bars) or 10 nM (filled bars) MeHg in DMEM. The significance of difference between two data sets was evaluated by the unpaired Student's t-test. ** - $p < 0.01$.

Figure 9

Effect of Hg^{2+} and MeHg on the viability of HEK 293 cells.

HEK 293 cells stably transfecting the $Ca_v3.1$ channel were treated with the control MEM, 1 μM of Hg^{2+} and 10 μM of MeHg for 10 min and 4 h, and the viability was assessed by MTT assay. Results are expressed as an absorbance measured at 540 nM in arbitrary units and represent the mean ± SEM of 6 measurements. The significance of difference between two data sets was evaluated by the unpaired Student's t-test. *** - $p < 0.001$.

Figure 10

Hg^{2+} and MeHg do not activate apoptosis or necrosis of HEK 293 cells.

FACS dot plots of cells maintained in MEM (a), cells exposed to MEM with 1 μM of Hg^{2+} (b) and cells exposed to MEM with 10 μM of MeHg (c) for 10 minutes (left column) or for 4 hours (right column). Apoptotic cells were stained by annexin V-FITC conjugate (y axes) and necrotic cells by propidium iodide (x axes). Each panel was divided into four quadrants: lower left – viable cells, lower right – necrosis, upper right – early apoptosis, upper right – late apoptosis and necrosis.

JPET Fast Forward. Published on December 2, 2005 as DOI: 10.1124/jpet.105.095463
This article has not been copyedited and formatted. The final version may differ from this version.

Table 1

Chronic effect of methylmercury on the $Ca_v3.1$ channel expressed in HEK 293 cells. Cells were cultured in MEM (see Materials and Methods) for 24 or 72 hours with or without addition of methylmercury to culture media. I-V relations from 15 cells cultured under each condition were measured, normalized with respect to cell capacity and averaged. Current densities evaluated at a peak of each I-V, i.e., at –30 mV, are summarized in the Table. Non-paired Students t-test was used for statistical comparison. n.s., not significant.

	1 nM MeHg			10 nM MeHg		
	$I_{control}$ pA/pF	I_{MeHg} pA/pF	Control vs. MeHg	$I_{control}$ pA/pF	I_{MeHg} pA/pF	Control vs. MeHg
24 hours	-97±8	-117±10	n.s.	-97±8	-90±9	n.s.
72 hours	-89±5	-111±6	$p<0.01$	-104±7	-88±6	n.s.

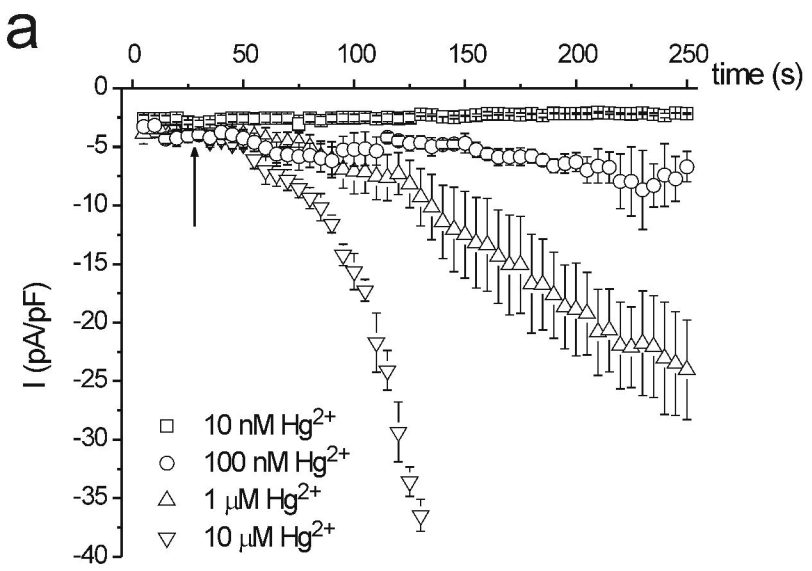

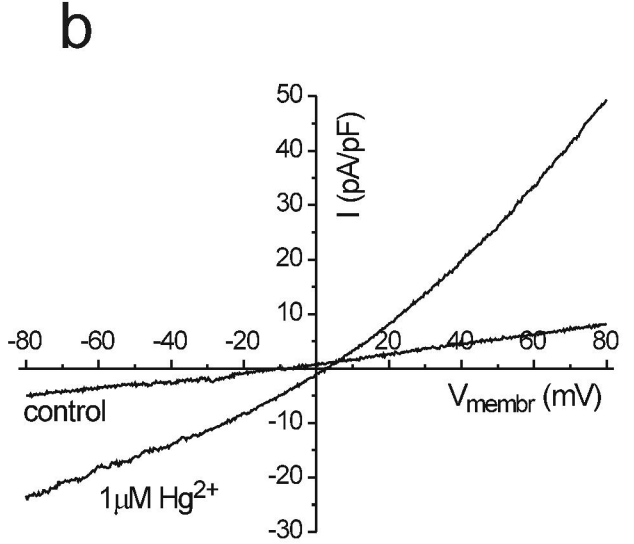

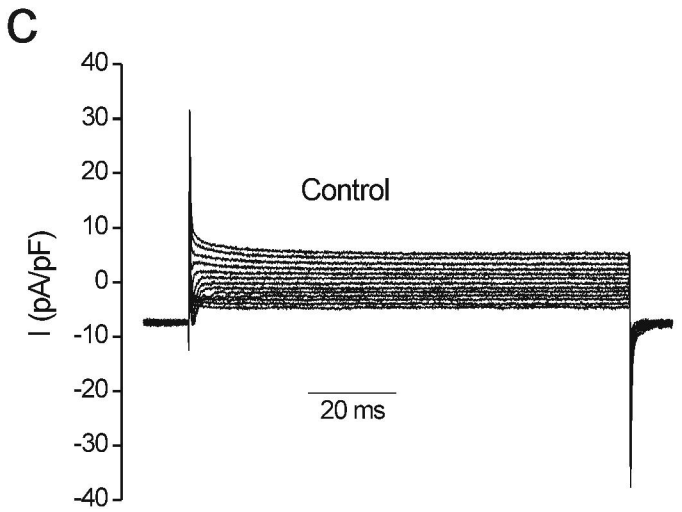

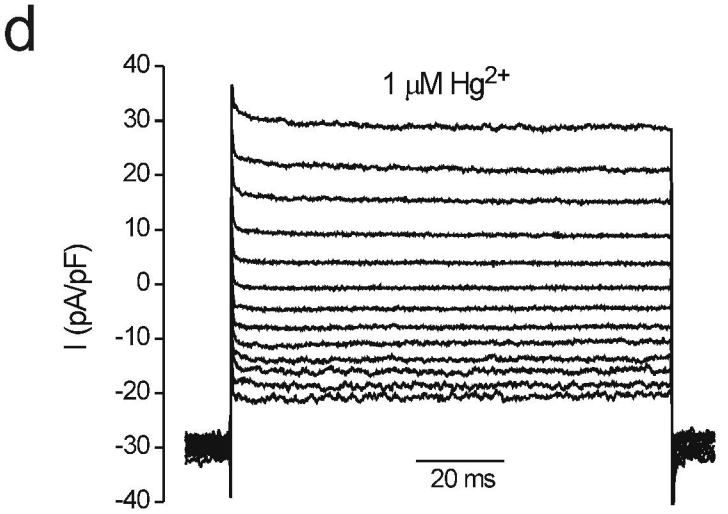

Fig 1

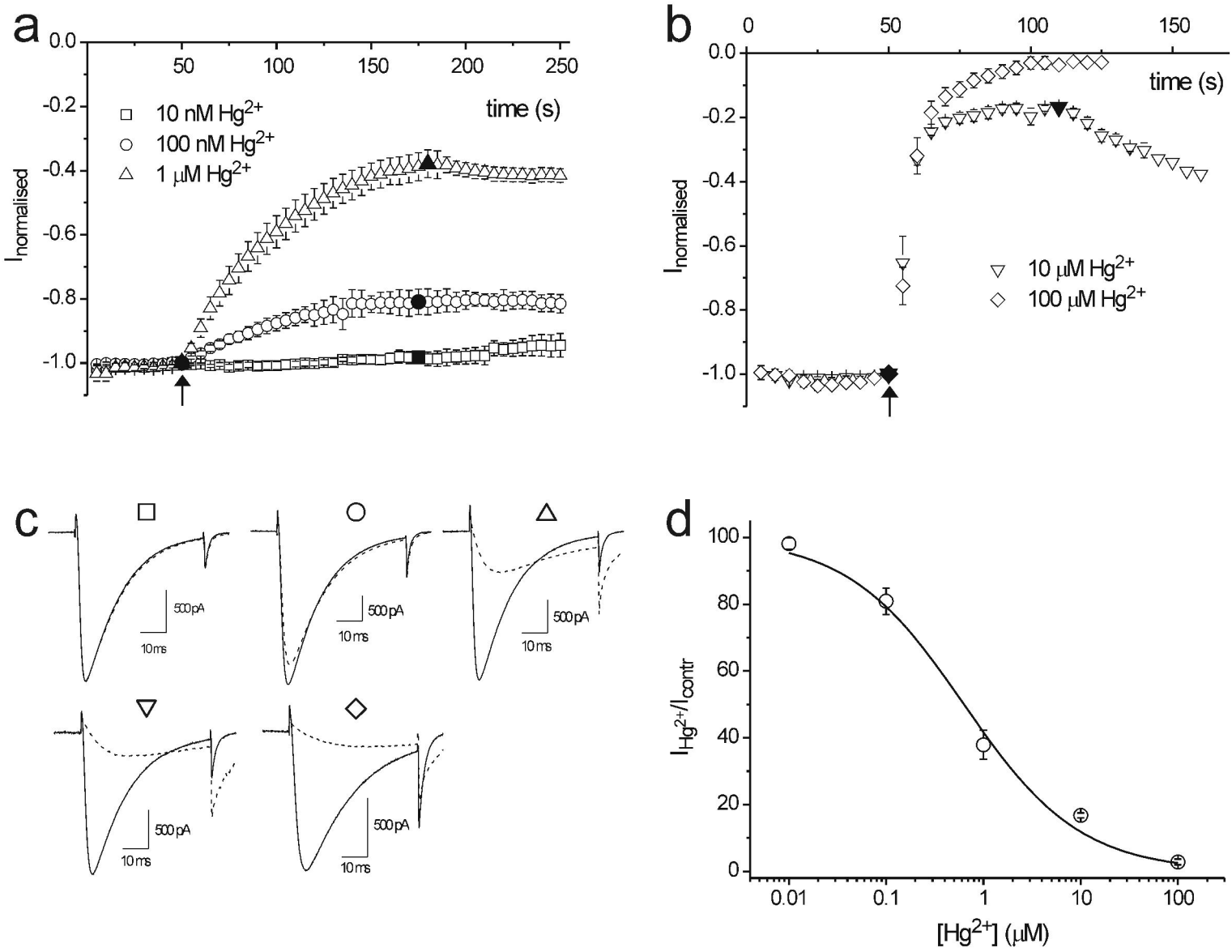

Fig 2

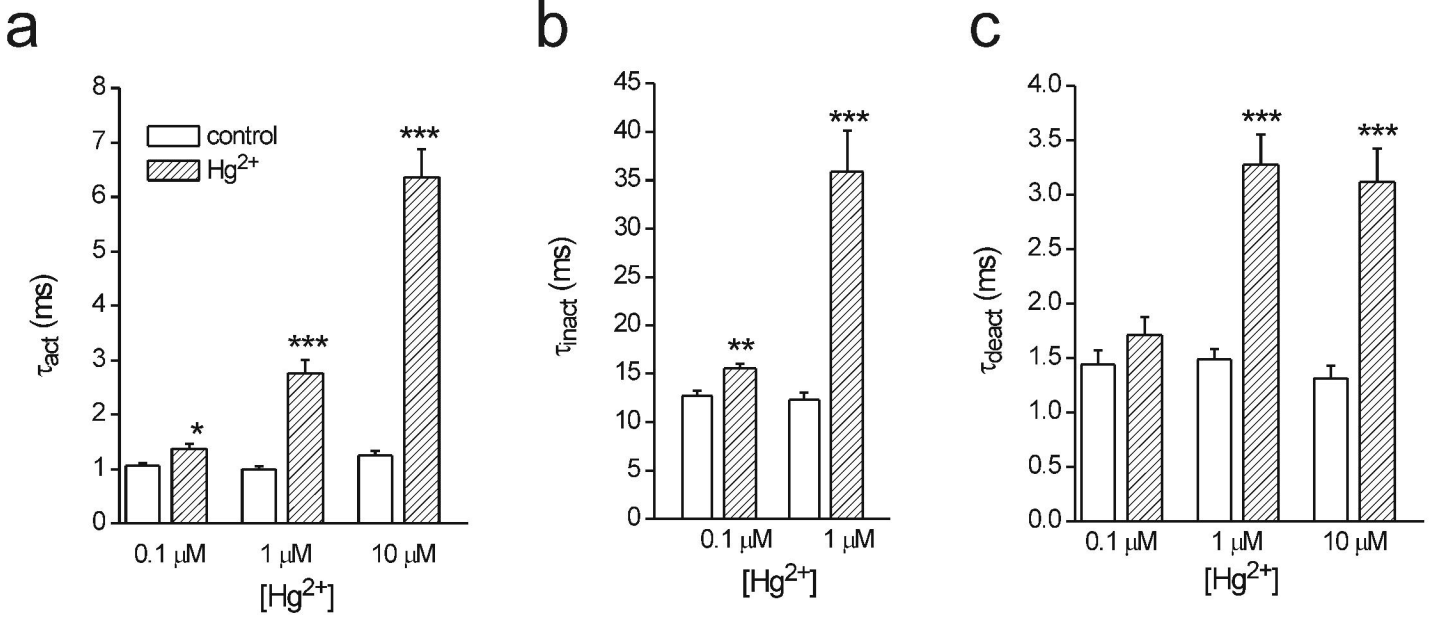

Fig 3

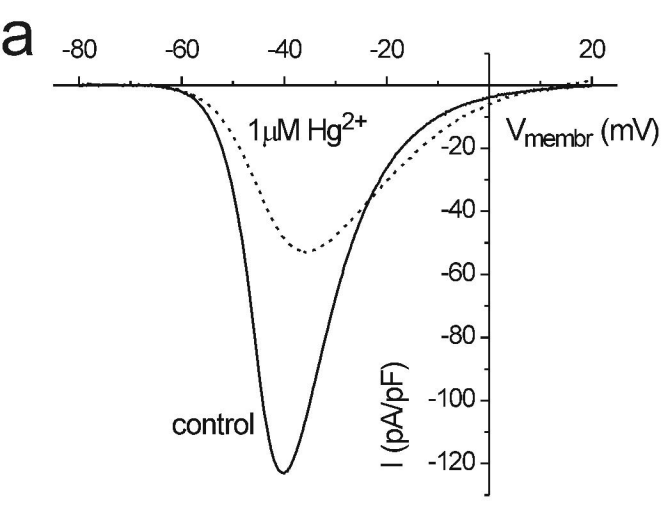
a
-80
-60
-40
-20
20
1μM Hg2+
Vmembr (mV)
-20
-40
-60
-80
-100
-120
control
I (pA/pF)

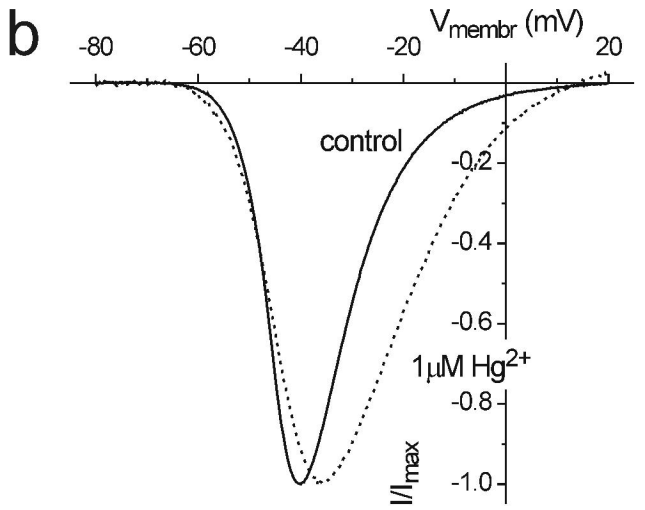
b
-80
-60
-40
-20
Vmembr (mV)
20
control
-0.2
-0.4
-0.6
1μM Hg2+
-0.8
-1.0
I/Imax

Fig 4

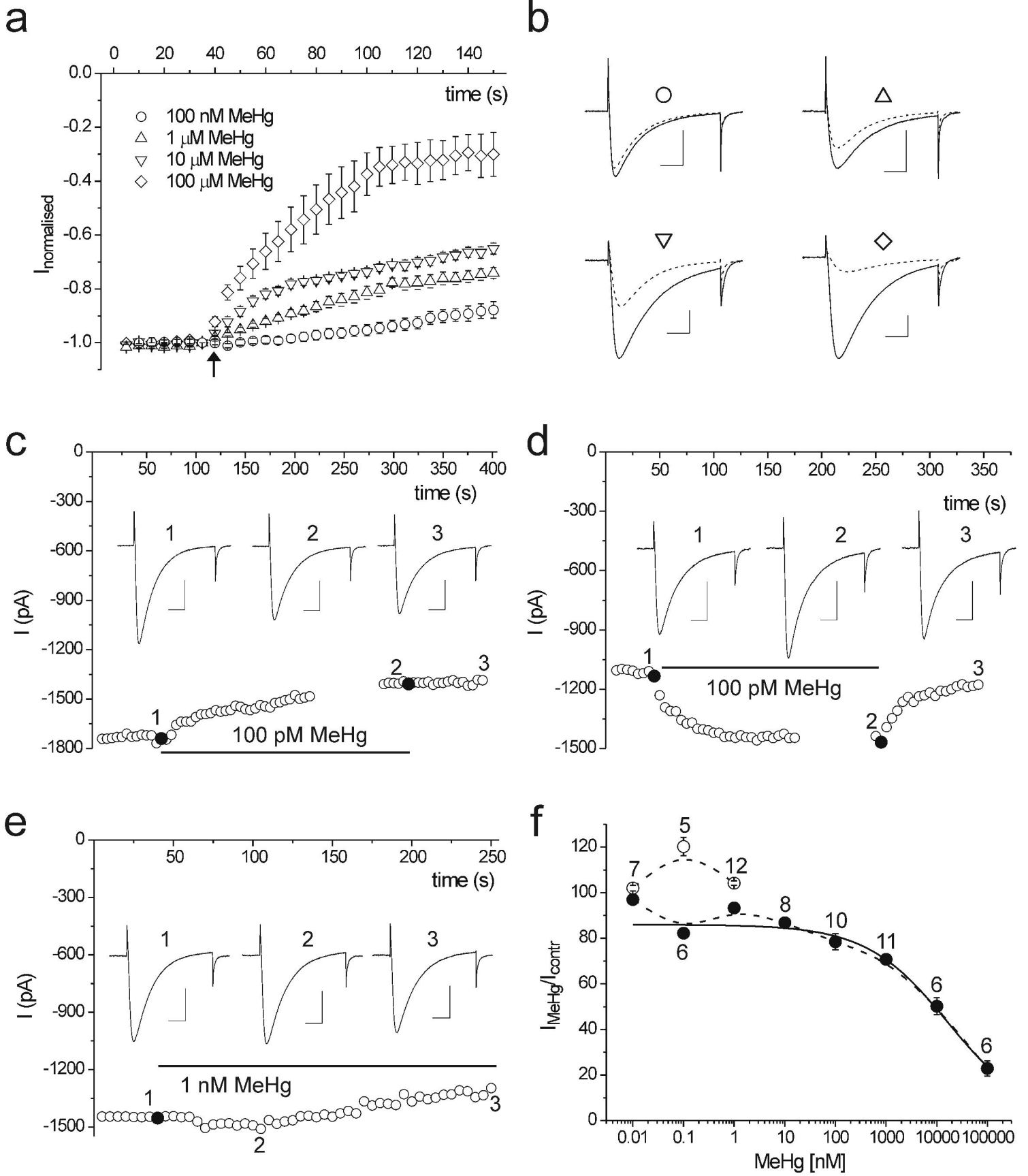
a
b
c
d
e
f
time (s)
100 nM MeHg
1 μM MeHg
10 μM MeHg
100 μM MeHg
I normalised
I (pA)
100 pM MeHg
1 nM MeHg
I MeHg/I contr
MeHg [nM]

Fig 5

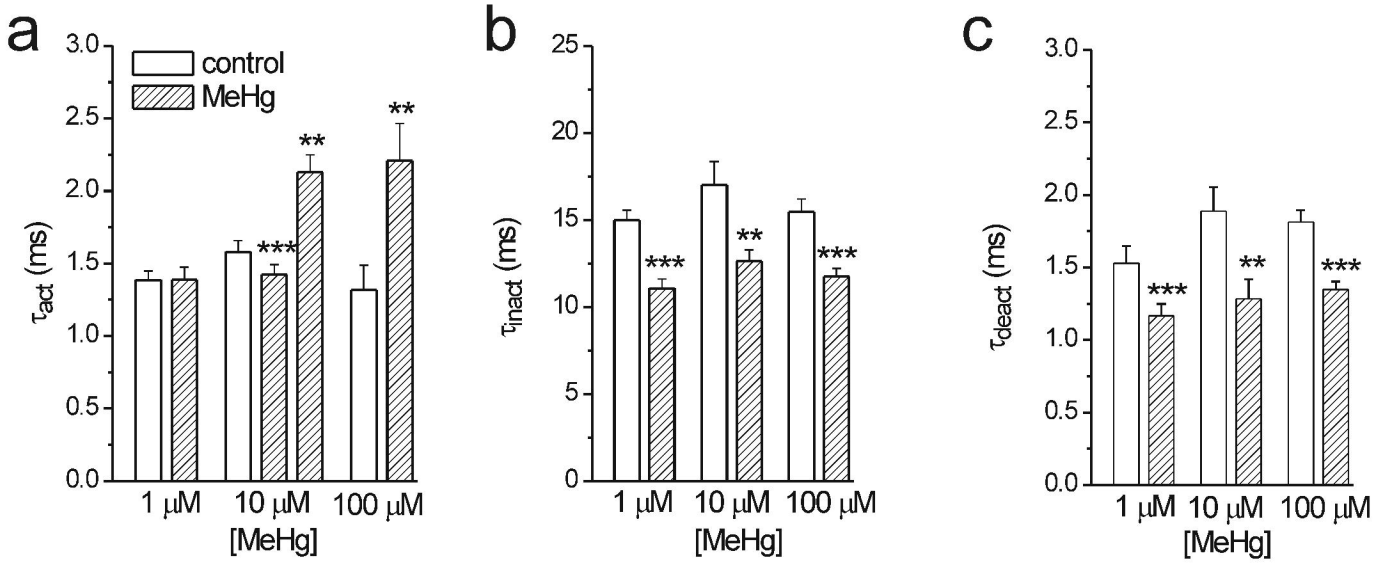
a
b
c
control
MeHg
τ_{act} (ms)
τ_{inact} (ms)
τ_{deact} (ms)
1 μM
10 μM
100 μM
[MeHg]
**
***

Fig 6

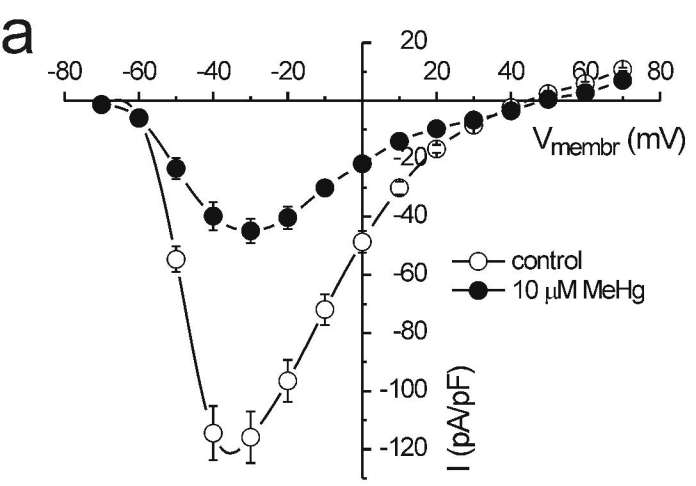
a
-80
-60
-40
-20
20
20
40
60
80
-20
-40
-60
-80
-100
-120
V membr (mV)
control
10 μM MeHg
I (pA/pF)

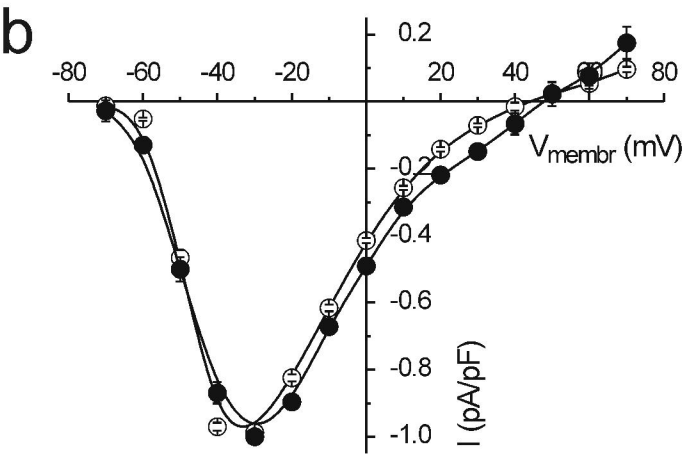
b
-80
-60
-40
-20
0.2
20
40
80
-0.2
-0.4
-0.6
-0.8
-1.0
V membr (mV)
I (pA/pF)

Fig 7

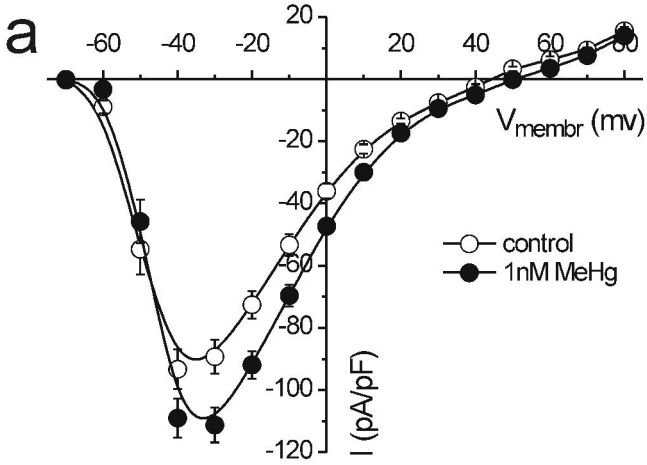
a
-60
-40
-20
20
40
60
80
20
-20
-40
-60
-80
-100
-120
V_{membr} (mv)
control
1nM MeHg
I (pA/pF)

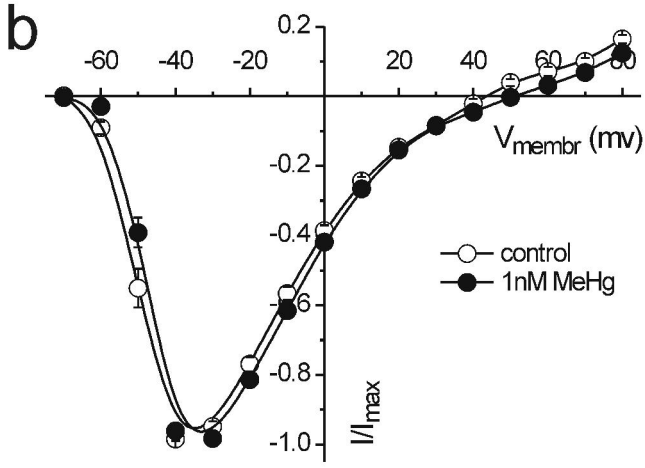
b
-60
-40
-20
20
40
60
80
0.2
-0.2
-0.4
-0.6
-0.8
-1.0
V_{membr} (mv)
control
1nM MeHg
I/I_{max}

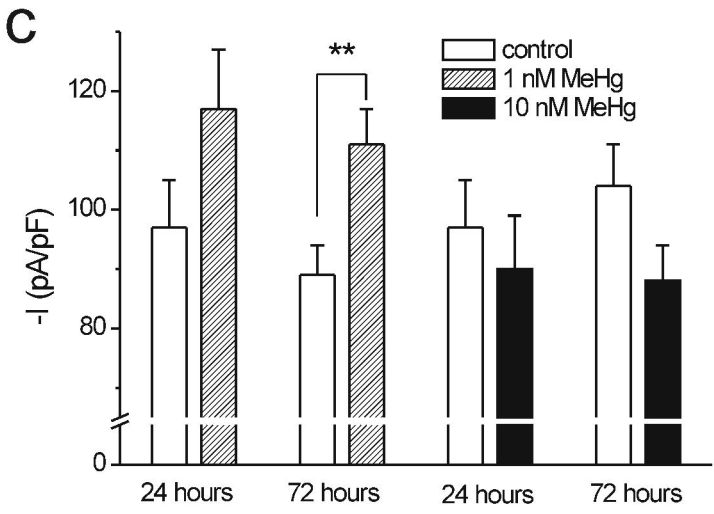
c
**
control
1 nM MeHg
10 nM MeHg
120
100
80
0
-I (pA/pF)
24 hours
72 hours
24 hours
72 hours

Fig 8

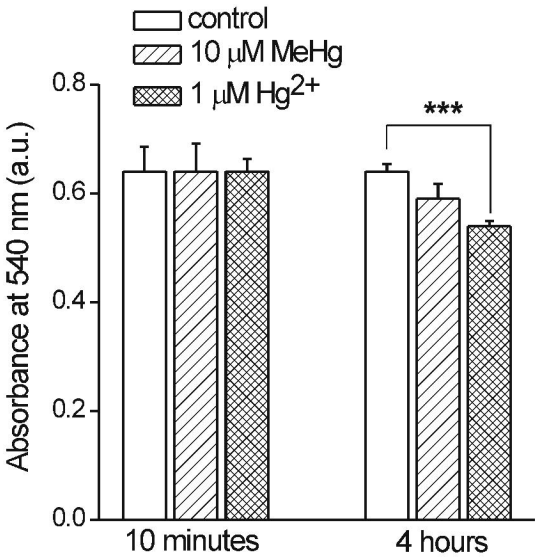
control
10 μM MeHg
1 μM Hg2+
***
Absorbance at 540 nm (a.u.)
0.8
0.6
0.4
0.2
0.0
10 minutes
4 hours

Fig 9

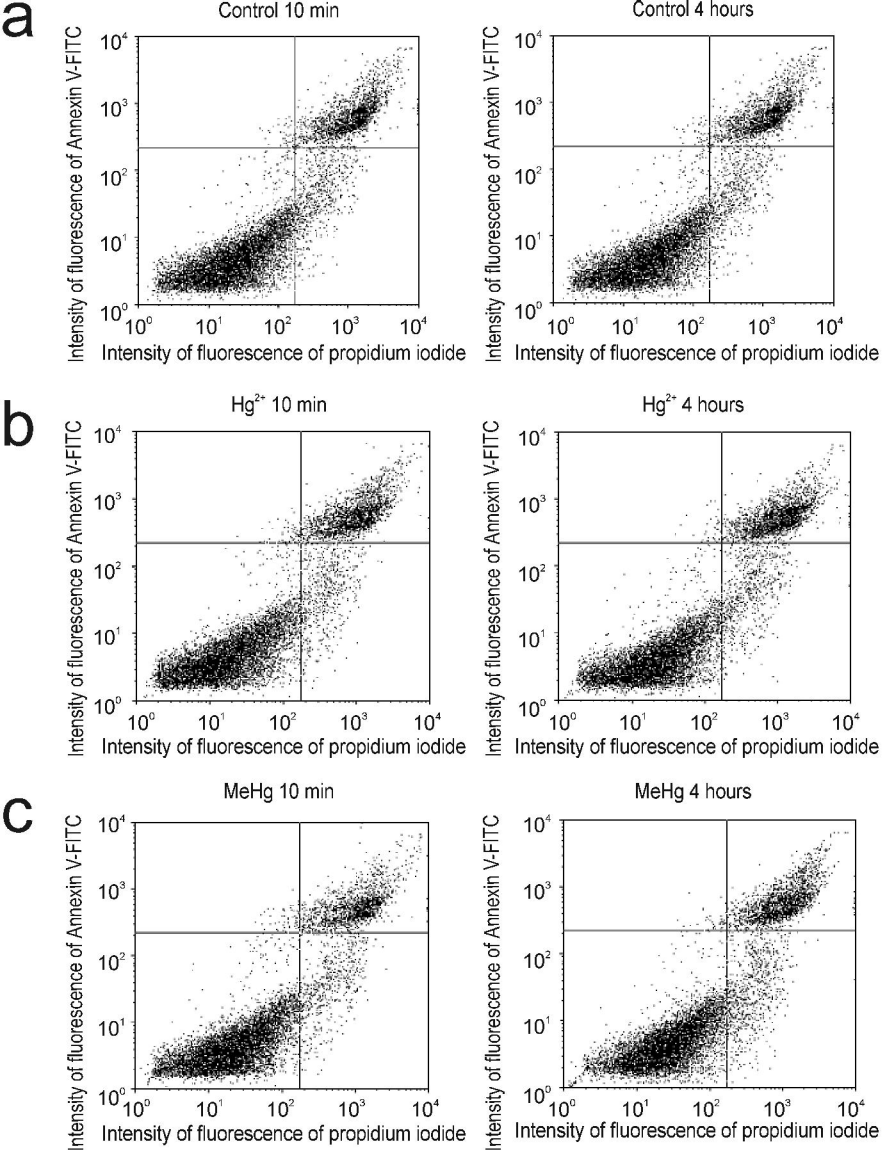
a
Control 10 min
Control 4 hours
b
Hg2+ 10 min
Hg2+ 4 hours
c
MeHg 10 min
MeHg 4 hours
Intensity of fluorescence of Annexin V-FITC
Intensity of fluorescence of propidium iodide
10^0
10^1
10^2
10^3
10^4

Fig 10